Preparation and Properties of PET/SiO_2 Composite Micro/Nanofibers by a Laser Melt-Electrospinning System

Xiuyan Li,[1] Huichao Liu,[1] Jiaona Wang,[1,2] Congju Li[1,2]

[1]*College of Materials Science and Engineering, Beijing Institute of Fashion Technology, Beijing 100029, China*
[2]*Beijing Key Laboratory of Clothing Materials R&D and Assessment, Beijing Institute of Fashion Technology, Beijing 100029, China*

Received 17 May 2011; accepted 29 September 2011
DOI 10.1002/app.36274
Published online 19 January 2012 in Wiley Online Library (wileyonlinelibrary.com).

ABSTRACT: Poly(ethylene terephthalate) (PET)/SiO_2 composite micro/nanofibers were successfully prepared by a laser melt-electrospinning system. The fibers with diameter ranging from 500 nm to 7 μm were obtained. The effect of laser current and applied voltage on the fibers morphologies was investigated by scanning electron microscopy (SEM), and the results showed that the relationship of process parameters and fibers diameter was complicated. The EDS analysis confirmed the presence of SiO_2 in the PET fibers matrix. The crystallization behavior of the electrospun PET/SiO_2 micro/nanofibers was investigated using X-ray diffraction (XRD) analysis and differential scanning calorimetry (DSC), and it was found that the as-electrospun fibers exhibited an amorphous phase. After heat-treatment at 120 and 160°C for 1 h, respectively, the fibers showed a high crystallinity. The thermal properties of fibers were studied using thermogravimetry-differential thermal analysis (TG–DTA), and showed the electrospun PET/SiO_2 composite fibers was not effective difference of thermostability compared with PET fibers when used for fibers materials.
 J Appl Polym Sci 125: 2050–2055, 2012

Key words: PET/SiO_2; laser melt electrospinning; fibers; electron microscopy; thermal properties

INTRODUCTION

Electrospinning provides an effective and versatile method to process solution or melt, mainly of polymers, into continuous fibers with diameters ranging from several micrometers down to a few nanometers.[1–3] Electrospinning is classified into solution and melt electrospinning. Compared to solution electrospinning, the melt electrospinning is currently under investigated but provides opportunities in numerous areas where solvent accumulation or toxicity are a concern.[4] Several reports have described the melt electrospinning in recent years.[5–14] However, there is another question that the molten polymer tents to degrade during the melting process. To minimize this degradation of the polymer, a method for rapid and uniform heating by irradiated the polymer with a CO_2 laser beam has been proposed. Many polymers have been successfully electrospun into nano or micron fibers by this technique.[15–21]

Recently, the organic–inorganic composite materials have attracted more and more attentions, because they can combine positive properties of organic and inorganic materials.[22] It can be widely used in many fields, such as optoelectronics, sensor technology, catalysis, filtration, and medicine. Several researchers made use of electrospinning technology to fabricate hybrid nanofibers based on polymeric and inorganic moieties.[23] Owing to the mild reactivity and well chemical properties, the SiO_2 nanoparticles are most widely used among the inorganic materials. Further, the PET/SiO_2 nanocomposite fibers have good thermal and chemical stability, excellent mechanical properties, and well dyeability.[24–29]

In this work, we attempted to prepare PET/SiO_2 composite fibers used a novel technology called laser melt electrospinning. We found that the micro/nanofibers were easily obtained by this method without especially skilled techniques. We also investigated the effect of the spinning parameters on the diameter of the electrospun fibers. In addition, the properties of the micro/nanofibers were investigated using scanning electron microscopy (SEM), energy dispersion spectroscopy (EDS), X-ray diffraction (XRD), differential scanning calorimetry (DSC), and

Correspondence to: C. Li (congjuli@gmail.com).
Contract grant sponsor: Natural Science Foundation of China; contract grant number: 51073005.
Contract grant sponsor: Beijing Natural Science Foundation; contract grant numbers: 2112013, KZ201010012012.
Contract grant sponsor: PHR (IHLB), the 863 Project; contract grant number: 2007AA021906.
Contract grant sponsor: Beijing Municipal Science and Technology Development Program, the 973 Project; contract grant number: 2010CB933501.

thermogravimetry-differential thermal analysis (TG–DTA).

EXPERIMENTAL

Materials

The intrinsic viscosity of the PET resins used in the present study was 0.6 d L/g and PET/SiO_2 (SiO_2: 4 wt %) composites were prepared using in situ polymerization, which was described elsewhere.[25]

PET rod-like samples, *ca.* 0.3 mm in diameter, were made using the melt flow indexer (XNR-450, China) at a temperature of 290°C and with a load of 1.2 kg. PET/SiO_2 rod-like samples also were fabricated according to this method, at a temperature of 262°C and with a load of 1.2 kg. These samples were provided for the laser melt electrospinning tests.

Laser melt-electrospinning equipment

Figure 1 shows a schematic diagram of the laser melt electrospinning system developed in our present study. A rod-like PET/SiO_2 sample was fed to the laser irradiating part; the feed rate was 6 mm/min. The end of the rod was melted by the irradiation of laser beams from three directions with an Onizca PIN-30R laser apparatus (Tokyo, Japan); the laser wavelength was 10.6 μm, the diameter of the laser spot was 5 mm, and the maximum power of the laser was 50 W. A high voltage was applied between the melted part of the rod and the grounded collector.

The diameter of the electrospun fibers may be controlled by many parameters such as laser current (L_c), applied voltage (V), and collector distance (C_d). Herein previous literature[15] and ours experiments, the diameter of electrospun PET/SiO_2 fibers was scarcely influenced by the collector distance, so the following tests were operated at a fixed collector distance (16 cm). Various combinations of process parameters were examined by changing L_c and V, one parameter at a time, for the following values: L_c = 15, 20, 25, 30, and 35 mA; and V = 5, 10, 15, 20, 25, and 30 kV.

Characterization

The morphologies and chemical analysis of the electrospun PET/SiO_2 fibers were characterized by scanning electron microscopy (SEM, JSM-6360LV, Japan) equipped with energy dispersion spectroscopy (EDS). Fiber samples were plated with a thin layer of gold before observation. The SEM images were analyzed with Smile View software (Provided with SEM, Japan) to determine average fibers diameter. The average diameter (AVG) and its standard deviation (SDEV) were calculated from 80 random measurements at each spinning condition.

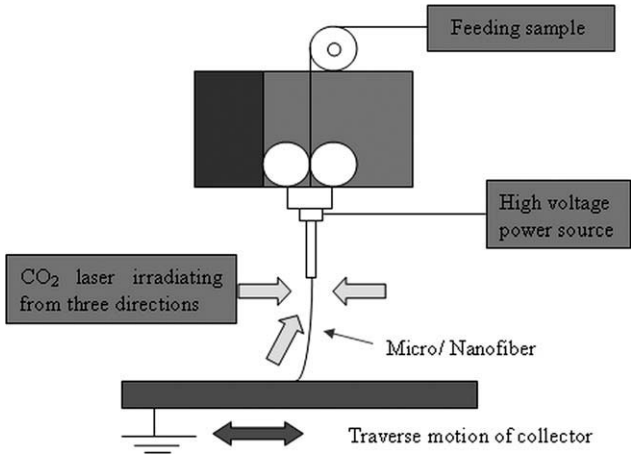

Figure 1 Schematic diagram of the Laser melt-electrospinning system developed in this work.

X-ray diffraction (XRD) analysis of electrospun PET and PET/SiO_2 fibers was performed on a D/max–rb diffractometer (Rigaku, Japan) using Cu K_α radiation at a scanning speed of 6°/min, and the scans were recorded at room temperature with 2θ ranging from 6 to 36°.

Differential scanning calorimetry (DSC) study of PET and PET/SiO_2 rod, and electrospun PET and PET/SiO_2 fibers was performed on EXSTAR DSC6200 (Seiko, Japan) in the ranging from room temperature to 300°C under nitrogen, a controlled heating rate was maintained at 10°C/min. The crystallization of the specimens was calculated according to the following equation:

$$\text{Crystallinity } (\%) = \frac{\Delta H_m - \Delta H_{cc}}{\Delta H_m^0} \times 100$$

where ΔH_m^0 is the melting enthalpy for a totally crystalline of PET, reported to 140 J/g.[30]

The thermal stability of electrospun PET and PET/SiO_2 fibers was examined using thermogravimetry-differential thermal analysis (TG–DTA) (TG/DTA6300, Japan) under nitrogen. The samples were ramped from room temperature to 600°C at a scanning rate of 10°C/min.

RESULTS AND DISCUSSION

Fiber morphology and diameter

PET/SiO_2 rod was successfully electrospun into ultrafine fibers in the range of 500 nm–7 μm with several morphologies. During our melt electrospinning, only a single polymer ejected was observed, while it is very common that the primary jet splits

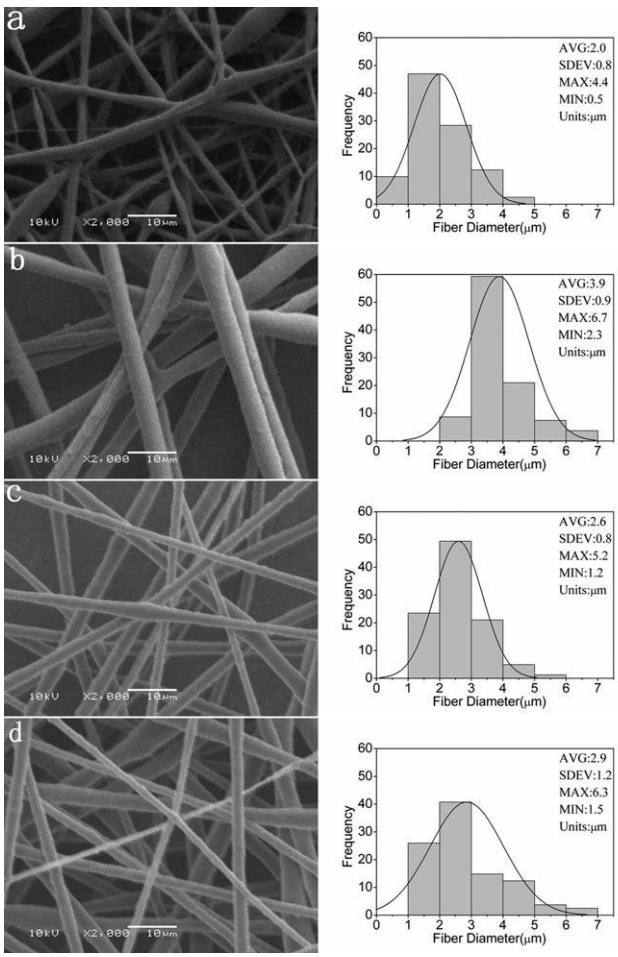

Figure 2 Representative SEM images and the diameter distribution of the electrospun PET/SiO_2 fibers: (a) $L_c = 25$ mA, $V = 5$ kV $C_d = 16$ cm; (b) $L_c = 30$ mA, $V = 25$ kV and $C_d = 16$ cm; (c) $L_c = 25$ mA, $V = 20$ kV and $C_d = 16$ cm; (d) $L_c = 25$ mA, $V = 25$ kV and $C_d = 16$ cm.

into multiple filaments in the solution electrospinning.[31] Figure 2 shows the representative images and the diameter distribution of the electrospun PET/SiO_2 fibers at different conditions in this experiment. Varied the applied voltages in the range of 5–30 kV at a constant laser current of 25 mA, we observed the fibers had non-homogeneous diameter at a low voltage of 5 kV, as shown in Figure 2(a). It is worth to note that spray-like particles can be seen at a low voltage, which may be ascribed to thermal decomposition of the polymer. When we raised the applied voltage or reduced the feeding speed, the spray-like particles disappeared and ultrafine fibers could be fabricated. However we tried to reduce the laser current, the spray phenomenon yet could be seen. We concluded that the electrical force was not sufficient to drive the melting cone which was irradiated by the laser beam, so that the melting cone cumulated excessive heat leading to degradation. As the applied voltage was further increased, a fiber jet was ejected from the melting cone.

The diameter of fiber segments had large variation along the length of the fiber. Figure 2(c,d) present the fibers morphology at the same laser current value as Figure 2(a), while not the same voltage value. In this case, the fibers had approximately symmetrical diameter of 2.6 ± 0.8 μm and 2.9 ± 1.2 μm, respectively. Broadly speaking, the increase in applied voltage slightly influences the electrospun fibers morphology, in the case of the voltage exceeded a critical value. A low voltage resulted in fibers with nonhomogeneous diameters, which may be attributed to low electrostatic force. It was not enough powerful to elongate the molten charged jets before it solidified. Compared Figure 2(b) with Figure 2(d), they were obtained at the same applied voltage and collector distance, varying laser current. The fibers diameter of the former was about 3.9 ± 0.9 μm. But this does not suggest that the higher laser current, the thicker fibers diameter. The fibers shown in figures just were some representatives of all the results. In facts, the fibers diameter took on fluctuations with an increase in laser current. It was also suggested there were some instability factors during the electrospinning process, such as accumulation of the static electricity, the variation of humidity, etc.

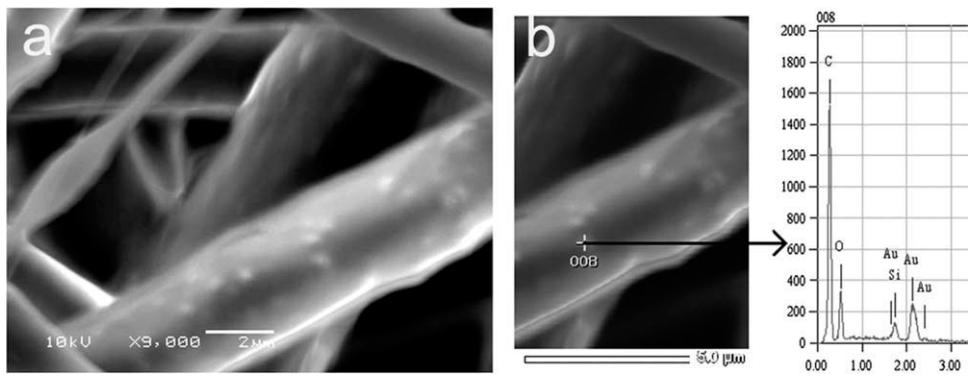

Figure 3 Typical EDS microanalysis on the selected spot of a single electrospun PET/SiO_2 fiber.

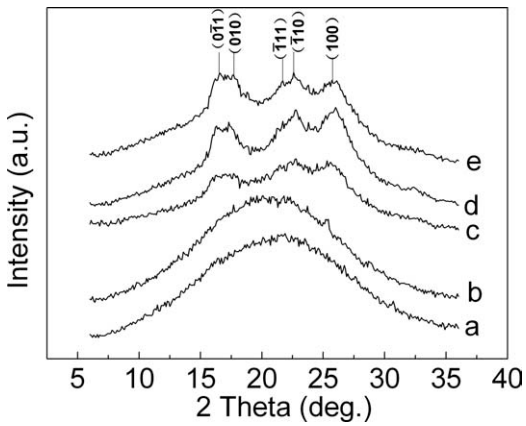

Figure 4 Typical XRD diffraction patterns of the electrospun PET and PET/SiO_2 fibers: (a) PET fibers; (b) PET/SiO_2 fibers; (c) PET/SiO_2 fibers annealing at 120°C; (d) PET/SiO_2 fibers annealing at 160°C; (e) PET fibers annealing at 160°C.

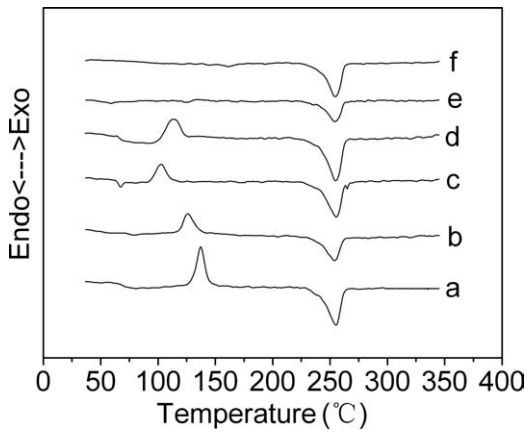

Figure 5 DSC thermograms of (a) PET rods; (b) electrospun PET fibers; (c) PET/SiO_2 rods; (d) electrospun PET/SiO_2 fibers; (e) electrospun PET/SiO_2 fibers annealing at 120°C; (f) electrospun PET/SiO_2 fibers annealing at 160°C.

As shown in Figure 3(a), the SiO_2 particles are dispersed well in PET fibers matrix. The diameters of particles are *ca.* 300 nm. The analysis of the chemical elements by EDS is shown in Figure 3(b), the element of Au came from the sputtering before SEM characterization. The element of silicon is confirmed with a peak in the spectra, other elements of carbon and oxygen are assigned to PET and/or SiO_2. This configuration of the fibers ensured that SiO_2 was mixed in the electrospun fibers.

In conclusion, the PET/SiO_2 hybrid micro/nanofibers were successfully produced by the laser melt electrospinning system, with diameter ranging from 500 nm to 7 μm.

Physical properties of the fibers

For a semicrystalline polymer, the crystal structure played an important role on the thermal and mechanical properties.[32] Generally, the rapid solidification of the polymer jet is accompanied by the rapid structure formation, which will lead to less developed structures in the fibers. As a result, most semicrystalline polymers have not enough time to form crystalline lamellae, which leads to lower crystallinity.[33] In this study, the electrospun fibers were annealed at 120 and 160°C for 1 h, respectively. Figure 4 shows XRD curves of the electrospun PET and PET/SiO_2 fibers at different processes. It can be seen that the as-electrospun PET and PET/SiO_2 fibers exhibit an amorphous phase, and there is no distinctive diffraction peak. This is may be attributed to undeveloped alignment of the polymer chains, which leads to lower crystallinity [Fig. 4(a,b)]. The influence of SiO_2 particles on the PET fibers can not be observed by XRD probably because of its low content. Under heat treatment at 120 and 160°C, respectively, the plot shows five diffraction peaks at 16.4, 17.6, 21.7, 22.8, and 25.9° in Figure 4(c), especially in Figure 4(d,e). These peaks corresponded to the (0 $\bar{1}$ 1), (0 1 0), ($\bar{1}$ 1 1), ($\bar{1}$ 1 0), and (1 0 0) diffraction planes of PET with the triclinic crystal.[30] The peak parameters, crystallite sizes and crystallinity of the electrospun PET and PET/SiO_2 fibers annealing at 160°C are listed in Table I. The crystallite sizes of PET/SiO_2 fibers for peaks (0 $\bar{1}$ 1), (0 1 0), ($\bar{1}$ 1 1), and (1 0 0) increased compared to that of PET fibers. The crystallinity of annealed PET/SiO_2 fibers also enhanced.

TABLE I
Peak Parameters, Crystallite Sizes, and Crystallinity of the Electrospun PET and PET/SiO_2 Fibers Annealing at 160°C (in a Triclinic Crystal Form)

Parameters	PET fibers annealing at 160°C	PET/SiO_2 fibers annealing at 160°C
2θ (deg.)		
0 $\bar{1}$ 1	16.4	16.3
0 1 0	17.6	17.4
$\bar{1}$ 1 1	21.7	21.5
$\bar{1}$ 1 0	22.8	22.7
1 0 0	25.9	26.0
Crystallite Size(Å)		
0 $\bar{1}$ 1	77.3	94.6
0 1 0	64.0	64.6
$\bar{1}$ 1 1	67.9	77.1
$\bar{1}$ 1 0	99.0	72.5
1 0 0	29.5	33.4
Crystallinity (%)	40.9	42.1

Figure 5 represents DSC thermograms of PET and PET/SiO_2 rods and electrospun fibers. The details of the thermal properties are shown in Table II. The melting temperature (T_m) of all the samples is *ca.* 255°C, there is little difference. The glass transition temperature (T_g) of the PET/SiO_2 rods and fibers was 63.4 and 66.9°C, which was lower than that of PET rods and fibers at 68.3 and 73.7°C, respectively. The cold crystallization temperature (T_{cc}) has an

TABLE II
Thermal Properties of PET and PET/SiO_2 Rods and Fibers

Rods/fibers	T_g (°C)	T_{cc} (°C)	T_m (°C)	ΔH_{cc} (J/g)	ΔH_f (J/g)	Crystallinity (%)
PET rods	68.3	137.2	255.2	37.2	49.5	8.8
PET fibers	73.7	125.9	254.1	41.1	57.4	11.6
PET/SiO_2 rods	63.4	102.8	255.5	22.0	59.2	26.6
PET/SiO_2 fibers	66.9	113.1	254.7	26.4	60.6	24.4
PET/SiO_2 fibers (annealing at 120°C)	48.6	N/A	254.1	N/A	56.3	40.2
PET/SiO_2 fibers (annealing at 160°C)	N/A	N/A	254.5	N/A	61.0	43.6

analogous regularity. The lower T_{cc} suggests a certain alignment of the polymer chains.[34] The crystallization of PET/SiO_2 rods and fibers are higher than that of PET rods and fibers. It indicated that SiO_2 particles exhibited strong nucleating effects, which effectively improved the nucleation and crystallization of the PET.[27] The results were identical to results obtained by XRD.

The cold crystallization peak occurred in both the rods and as-electrospun fibers [Fig. 5(a–d)]. With annealing treatment at 120 and 160°C, the peak of cold crystallization disappeared due to the easier motion of the polymer chains [Fig. 5(e,f)]. Moreover, with the increase of annealing temperature, the annealed PET/SiO_2 fibers have the crystallinity of 40.2% at 120°C and 43.6% at 160°C, respectively, compared with 24.4% of as-electrospun fibers. It also indicated undeveloped structures existed in the as-electrospun fibers. These features occurring in the electrospun fibers on heating are a signature of the rapid structure formation during the electrospinning process.[35]

TG thermograms of the electrospun PET/SiO_2 and pure PET fibers are shown in Figure 6. The onset decomposition temperature for PET fibers was approximately 400°C, while for PET/SiO_2 fibers the temperature was about 408°C, there was a slight increase. However, it is not practical difference of thermostability when used for fibers materials.

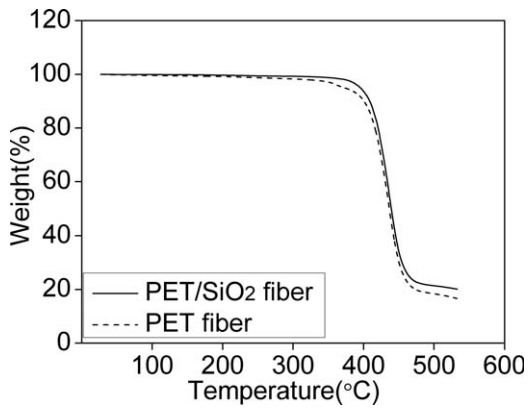

Figure 6 Thermograms for the electrospun PET and PET/SiO_2 fibers (Dashed lines represent PET fiber; solid lines represent PET/SiO_2 fibers).

CONCLUSIONS

The PET/SiO_2 composite fibers with diameter ranging from 500 nm to 7 μm have been successfully spun by laser melt electrospinning. According to our experimental observation, only a molten ejected was formed in the process, and electrically driven bending instability of the molten jet was not to emerge. The applied voltage and the laser current did not particularly affect the fibers diameter. The PET/SiO_2 hybrid fibers were verified by EDS. The XRD and DSC analyses showed the electrospun PET/SiO_2 composite fibers had undeveloped molecule structures. Thermal treatment can be used to enhance the crystallinity of the electrospun PET/SiO_2 fibers. The TG thermal analysis exhibited the electrospun PET/SiO_2 composite fibers was not effective difference of thermostability compared with PET fibers when used for fibers materials.

References

1. Greiner, A.; Wendorff, J. H. Angew Chem Int Ed 2007, 46, 5670.
2. Li, D.; Xia, Y. N. Adv Mater 2004, 16, 1151.
3. Huang, Z. M.; Zhang, Y. Z.; Kotaki, M.; Ramakrishna, S. Compos Sci Technol 2003, 63, 2223.
4. Hutmacher, D. W.; Dalton, P. D. Chem Asian J 2011, 6, 44.
5. Lyons, J. Ph.D. Thesis, Drexel University: PA, USA, 2004.
6. Lyons, J.; Li, C.; Ko, F. Polymer 2004, 45, 7597.
7. Dalton, P. D.; Calvet, J. L.; Mourran, A.; Klee, D.; Möller, M. Biotechnol J 2006, 1, 998.
8. Dalton, P. D.; Klinkhammer, K.; Salber, J.; Klee, D.; Möller, M. Biomacromolecules 2006, 7, 686.
9. Dalton, P. D.; Grafahrend, D.; Klinkhammer, K.; Klee, D.; Möller, M. Polymer 2007, 48, 6823.
10. Dalton, P. D.; Joergensen, N. T.; Groll, J.; Möller, M. Biomed Mater 2008, 3, 1.
11. Deng, R. J.; Liu, Y.; Ding, Y. M.; Xie, P. C.; Luo, L.; Yang, W. M. J Appl Polym Sci 2009, 114, 166.
12. Wang, X. F.; Huang, Z. M. Chin J Polym Sci 2010, 28, 45.
13. Zhou, H. J.; Green, T. B.; Joo, Y. L. Polymer 2006, 47, 7497.
14. Detta, N.; Brown, T.; Edin, F. K.; Albrecht, K.; Chiellini, F.; Chiellini, E.; Dalton, P. D.; Hutmacher, D. W. Polym Int 2010, 59, 1558.
15. Ogata, N.; Yamaguchi, S.; Shimada, N.; Lu, G.; Iwata, T.; Nakane, K.; Ogihara, T. J Appl Polym Sci 2007, 104, 1640.
16. Ogate, N.; Shimada, N.; Yamaguchi, S.; Nakane, K.; Ogihara, T. J Appl Polym Sci 2007, 105, 1127.
17. Ogata, N.; Lu, G.; Iwata, T.; Yamaguchi, S.; Nakane, K.; Ogihara, T. J Appl Polym Sci 2007, 104, 1368.

18. Shimada, N.; Tsutsumi, H.; Nakashi, K.; Ogihara, T.; Ogata, N. J Appl Polym Sci 2010, 116, 2998.
19. Nakata, K.; Kinugawa, S.; Takasaki, M.; Ohkoshi, Y.; Gotoh, Y.; Nagura, M. Sen-i Gakkaishi 2009, 65, 257.
20. Tian, S.; Ogata, N.; Shimada, N.; Nakane, K.; Ogihara, T.; Yu, M. J Appl Polym Sci 2009, 113, 1282.
21. Takasaki, M.; Fu, H.; Nakata, K.; Ohkoshi, Y.; Hirai, T. Sen-i Gakkaishi 2008, 64, 29.
22. Agag, T.; Tsuchiya, H.; Takeichi, T. Polymer 2004, 45, 7903.
23. Yuan, J.; Muller, A. Polymer 2010, 51, 4015.
24. Paul, D. R.; Robeson, L. M. Polymer 2008, 49, 3187.
25. Yang, Y.; Gu, H. J Appl Polym Sci 2007, 105, 2363.
26. Yang, Y.; Gu, H. J Appl Polym Sci 2006, 102, 3691.
27. Yang, Y.; Xu, H.; Gu, H. J Appl Polym Sci 2006, 102, 655.
28. Cheng, S.; Shen, D.; Zhu, X.; Tian, X.; Zhou, D.; Fan, L. J. Eur Polym J 2009, 45, 2767.
29. Kim, Y. J.; Ahn, C. H.; Choi, M. O. Eur Polym J 2010, 46, 1957.
30. Leung, F. K. P.; Cheung, W. L.; Lin, X. D.; Jia, D.; Chung, C. Y. J Appl Polym Sci 2007, 104, 137.
31. Shin, Y. M.; Hohman, M. M.; Brenner, M. P.; Rutledge, G. C. Appl Phys Lett 2001, 78, 1149.
32. Pan, P.; Kai, W.; Zhu, B.; Dong, T.; Inoue, Y. Macromolecules 2007, 40, 6898.
33. Baja, A.; Main, Y. W.; Wong, S. C.; Abtahi, M.; Chen, P. Compos Sci Technol 2010, 70, 703.
34. Mo, X.M.; Xu, C.Y.; Kotaki, M.; Ramakrishna, S. Biomaterials 2004, 25, 1883.
35. Greiner, A.; Wendorff, J. H. Adv Mater 2001, 13, 70.